Journal of GeoEngineering, Vol. 14, No. 2, pp. 53-64, June 2019
http://dx.doi.org/10.6310/jog.201906_14(2).1

SEISMIC EARTH PRESSURE COMPUTATION USING MODIFIED DUBROVA'S MODEL

Amol Maskar [1*] and Suhasini Madhekar [2]

ABSTRACT

The design of a retaining wall needs complete knowledge of the earth pressure behind it for both active and passive conditions. In case of earthquake events, the design requires special attention to reduce the devastating effects. Under seismic condition, the available literature mostly focuses on pseudo-static and pseudo-dynamic methods, to evaluate the seismic earth pressure. However, these methods do not incorporate the effect of wall movement on the earth pressure distribution. Dubrova was the first to consider such effect. In this paper, modified Dubrova's model based on redistribution principle (considering seismic effect) has been developed. The model is used to determine the nonlinear distribution of active earth pressure acting on a retaining wall, by considering various modes of wall movement. For checking the accuracy and applicability of the predictions using the modified Dubrova's model, equations of active earth pressure are compared to the available experimental results for retaining walls, considering variation in height, soil friction angle, wall friction angle, and seismic acceleration coefficient. The modified Dubrova's model considers both nonlinear static and nonlinear seismic earth pressure distributions. Parametric studies are performed to study the distribution of seismic earth pressure along the height of a retaining wall. It is found that the maximum earth pressure occurs between 0.35 H to 0.40 H above the wall base (H is the height of the mat). Results obtained using modified Dubrova's model are in good agreement with experimental results of Tsagareli and others. Present study gives 25% higher earth pressure compared to Tsagareli's method, whereas 30% higher earth pressure compared to Ghazavi and Yeganeh's method. Though seismic earth pressure obtained by all above approaches and that obtained by modified Dubrova's model has different formulation background, the final earth pressure distribution is approximately of the same nonlinear nature.

Key words: Seismic active earth pressure, modified Dubrova's model, pseudo-static methods, pseudo-dynamic methods, nonlinear distribution, redistribution principle.

1. INTRODUCTION

An estimation of the active and passive earth pressures acting on retaining walls is of vital importance in geotechnical design. Coulomb's theory (Coulomb 1776) is generally used to calculate active and passive earth pressure, which considers wall friction angle (δ). However, the distribution of active and passive earth pressure behind the wall obtained from Coulomb (1776) is linear, which is not consistent with the experimental results given by Tsagareli (1965) and Tang (1988). This is because of the arching effect on the retained soil, which is attributed to the frictional resistance between the wall and the backfill. The study of seismic active earth pressure is an important topic of research for safe design of retaining wall in different seismic zones. The pioneering work on earthquake induced lateral earth pressure under active and passive conditions behind retaining wall is reported by Mononobe and Matsuo (1929) and Okabe (1924). Currently, the pseudo-static approach which follows Coulomb's static earth pressure analysis, known as Mononobe-Okabe's method (Kramer 1996) is used to evaluate the seismic earth pressure. Recent works of Richards and Chi (1994), Subba Rao and Choudhury (2005), Choudhury and Nimbalkar (2006), and Choudhury and Singh (2006) have considered the pseudo-static approach to evaluate seismic active earth pressure. Further, Choudhury and Nimbalkar (2006) and Choudhury *et al.* (2014) studied a pseudo dynamic approach for evaluation of seismic active earth pressure on the rigid retaining wall, considering different boundary conditions. However, both pseudo-static and pseudo-dynamic approaches do not consider the effect of wall movement on the earth pressure distribution. Dubrova (1963) presented an analytical method in the form of redistribution principle, which is based on different wall movements like rotation at the top, rotation at the bottom and pure translation (Fig. 1), to calculate static earth pressure. The distribution of static earth pressure was found to be parabolic, which matches with experimental results given by Tsagareli (1965) and Tang (1988). In the present study, the redistribution principle with the incorporation of seismicity effect is developed, and seismic active earth pressure distribution behind retaining wall based on the modified Dubrova's model is evaluated. The present study represents the distribution of lateral earth pressure due to static and seismic loading behind a rigid retaining wall using a closed form solution. The differential equation governing an arbitrary element at a given depth along the wall height has been derived and solved using appropriate boundary conditions. In this paper, an analytical solution based on redistribution principle is presented, in which a straight failure surface is considered in cohesionless backfill behind a rigid retaining wall. The formulation for lateral seismic earth pressure distribution on the wall is developed. The results obtained from the present study are compared with the experimental and analytical

Manuscript received October 27, 2017; revised October 9, 2018; accepted November 13, 2018.
[1*] Research Scholar (corresponding author), Department of Civil Engineering, College of Engineering, Pune (COEP), Pune 411005, India (e-mail: amol.maskar5@gmail.com).
[2] Associate Professor, Applied Mechanics, College of Engineering, Pune (COEP), Pune 411005, India.

results given by Tsagareli (1965), Tang (1988), Wang *et al.* (2004), Goel and Patra (2008), Ghazavi and Yeganeh (2011), and Rao and Chen (2015). The present results are found to be in good agreement with those presented by these researchers.

2. MODIFIED DUBROVA'S MODEL

Coulomb (1776) provided no analytical basis for the distribution of earth pressure behind the retaining wall. He assumed the pressure distribution to be quasi-hydrostatic and considered the resultant earth force acting at one-third of the height of the wall. Results of large scale model tests by Terzaghi (1943) have demonstrated the validity of these distributions for very rigid retaining walls with sand backfills that evidence a rotation about their toe. For other modes of movement, such as rotation about the top or about the center of a wall or translation movements, test results indicate parabolic distribution of pressures. Although the mechanism responsible for these differences is still imperfectly understood, it is universally agreed that the pressure distribution on lateral supports is dependent on the nature and degree of movement permitted after the backfill is placed. Within this framework, the difference between the distribution of pressures for rigid retaining walls and flexible retaining walls is simply a function of displacement that is permitted over the height of wall.

A relatively little known procedure that appears to have considerable merit for determining the pressure distributions is explained in the paper. The method of redistribution of pressure, *i.e.,* redistribution principle, was first proposed by Dubrova (1963) and was also described later by Harr (1966) and Das (2007). The principle gives the distribution of earth pressure, according to various wall movements, *i.e.,* rotation at the top, rotation at the bottom, and pure translation. The solution by Dubrova assumes the validity of Coulomb's solution. The Dubrova's model based on redistribution principle can be understood from Fig. 1, in which Fig. 1(a) indicates retaining wall rotates about the base, Fig. 1(b) indicates retaining wall rotates about the top, whereas Fig. 1(c) shows the pure translation (earth pressure is approximately the same as that of existing methods, and its distribution is parabolic), which is the combination of rotation of the top and rotation at the bottom. The variation of active earth pressure over the depth of the wall indicates parabolic earth pressure distribution. Various rupture lines are shown in Fig. 4 in which resultant F_i makes an angle $-\psi$ to $+\psi$ with the normal drawn to the rupture lines.

According to Bang (1985), the method of redistribution of pressure for active case estimates the magnitude and distribution of the lateral earth pressure exerted by cohesionless soil behind the rigid retaining wall, experiencing outward tilt about its base from an initial active state to a full active state. The initial active state refers to a stage of wall tilt when only the soil element on the ground surface experiences a sufficient lateral movement to achieve an active condition. The full active state occurs when all soil elements from the ground surface to the base of the wall are in active condition. As per Dubrova's hypothesis, between these two extremes, intermediate active states exist. The transition of the lateral earth pressures from an initial active state to a full active state is discussed as below.

Figure 2 shows free body diagram of the sliding wedge in which W is self-weight of the wedge, P_a is active earth thrust, F is the resultant force, ϕ is the soil friction angle, δ is wall friction angle, and ψ is an orientation angle. z is any downward depth from the top of the wall which is zero at top and H at the bottom as shown in Fig. 3. The angle, π, representing the direction of the force, F, is equal to the soil friction angle, ϕ, according to Coulomb's theory, when the soil mass is in active condition. The angle, ψ, however, may be less than the soil friction angle, ϕ, when the soil mass is yet to be in active condition. The concept was first proposed by Dubrova (1963) in her method of redistribution of pressure. This observation leads to the following assumptions:

1. At initial active state, *i.e.,* when the active condition occurs only at $z = 0$, $\psi = \phi$ at $z = 0$ and $\psi = 0$ at $z = H$, as shown in Fig. 3(a).
2. At full active state, *i.e.,* when an active condition exists along the entire depth of the wall, $\psi = \phi$ everywhere as shown in Fig. 3(b). Therefore, at any intermediate active state, the variation of the angle, ψ, could be assumed as $\psi = \phi$ at $z = 0$ and $\psi = 0$ at $z = H$ with linear variation. The lateral earth pressure at any depth and at any intermediate active state can be obtained by differentiating the thrust, P_a, with respect to depth, z. According to Dubrova's hypothesis, the wall friction angle, δ, is a function of the soil friction angle, ϕ, rather than a function of the orientation angle, ψ.

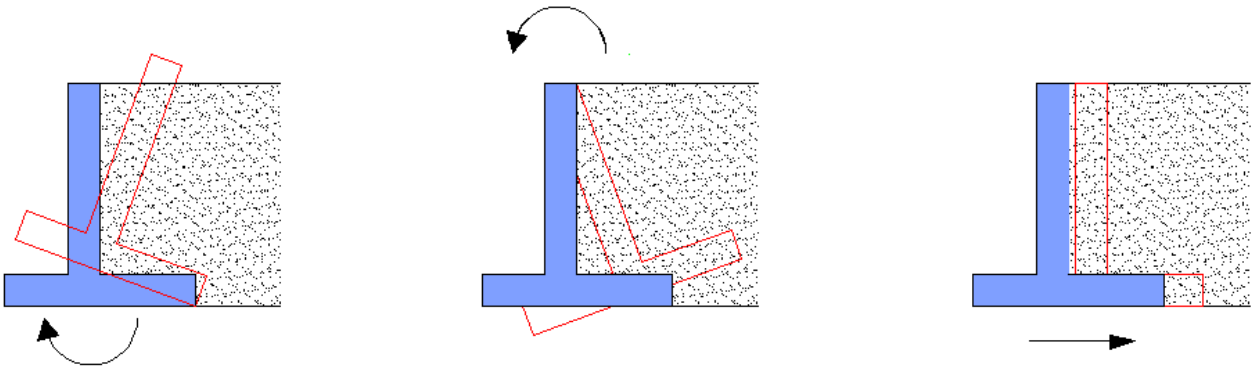

(a) Rotation at bottom (b) Rotation at top (c) Pure translation

Fig. 1 Various modes of wall movements

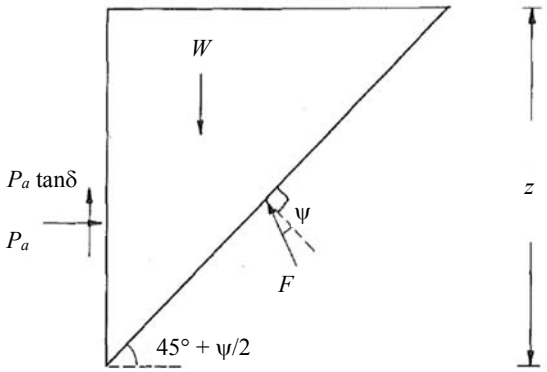

Fig. 2 Free body diagram of the sliding wedge (Bang, 1985)

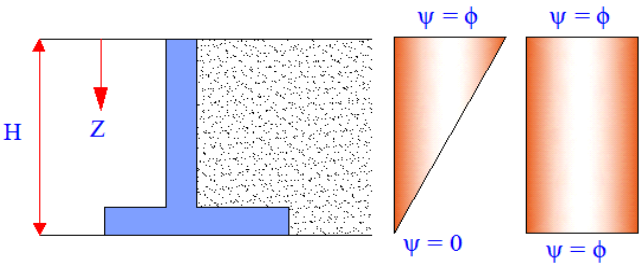

(a) At initial active state (b) At full active state

Fig. 3 Variation of ψ with depth

3. MATHEMATICAL MODEL

Figure 4 shows that retaining wall rotates about point O. At each point of the wall there is a corresponding failure plane. F_i is the resultant of normal and frictional forces acting on failure plane and is inclined at an angle of ψ to the normal. OA is pushed into soil, whereas OB is pulled outward, as shown in Fig. 4. Hence, there are limiting active and passive conditions only at bottom and top of the wall, respectively. The force F_i is inclined at an angle – ϕ at top and + ϕ at bottom; while in-between, values of ϕ are linearly distributed. Dubrova (1963) assumed Coulomb's theory and replaced ϕ by ψ(z), which considers soil friction angle from – ϕ to + ϕ for $z = 0$ and $z = H$, respectively.

A single failure plane, on which various forces act, is shown in Fig. 5, where k_h is a horizontal seismic acceleration coefficient and P_d is the active thrust (kN/m) inclined to the horizontal at an angle δ. Generally due to earthquake, retaining wall deflects more about horizontal axis than that of vertical axis hence k_v is not considered.

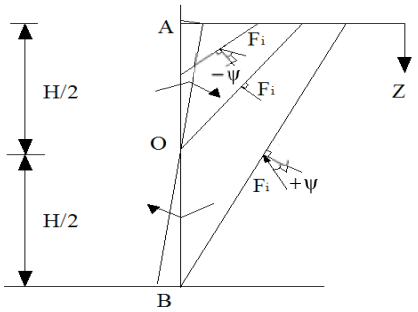

Fig. 4 Resultant force acting on failure plane

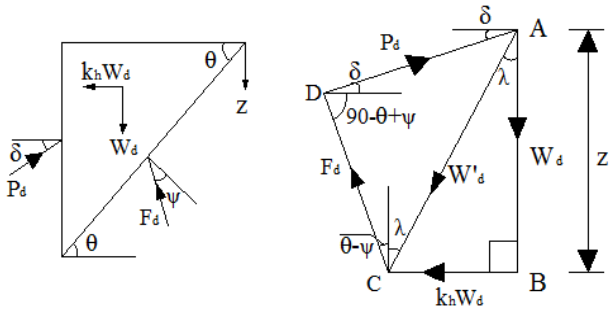

(a) Trial wedge of retaining wall (b) Force polygon

Fig. 5 Single failure plane of retaining wall

3.1 Seismic Active Earth Thrust

To determine seismic active earth thrust behind the retaining wall, a force polygon from the trial wedge is considered as shown in Figs. 5(a) and 5(b). Generally due to earthquake, the retaining wall deflects more about horizontal axis and less about vertical axis. Therefore, Fig. 5 (a) does not consider vertical seismic coefficient k_v. The polygon consists of seismic active earth thrust P_d, weight of trial wedge W_d, inertia force k_hW_d, and resultant force on trial wedge F_d. Also, W_d' is the resultant of weight of wedge (W_d) and the inertia force (k_hW_d).

From the force polygon shown in Fig. 5(b), using sine rule, the following expression can be obtained:

$$\frac{P_d}{\sin(\theta-\psi+\lambda)} = \frac{W_d'}{\sin[90°-(\theta-\psi-\delta)]} = \frac{F_d}{\sin[90°-(\delta+\lambda)]} \quad (1)$$

The resultant W_d' is given by cosine rule:

$$W_d' = \sqrt{(W_d)^2 + (k_h W_d)^2 + 2(W_d)(k_h W_d)\cos\theta} \quad (2)$$

As θ = 90°, cos (90°) = 0

$$W_d' = \sqrt{(W_d)^2 + (k_h W_d)^2}$$

$$W_d' = W_d\sqrt{1+(k_h)^2} \quad (3)$$

If z is the height of the wedge and γ is the unit weight of backfill, the weight of the wedge is given by

$$W_d = 0.5\,\gamma z^2 \cot\theta \quad (4)$$

Also, $\lambda = \tan^{-1}(k_h/(1+k_v))$, where k_v is vertical seismic coefficient. From Eq. (1), the seismic active earth thrust (P_d) is given by

$$P_d = \frac{W_d'\,\sin(\theta-\psi+\lambda)}{\sin[90°-(\theta-\psi+\lambda)]} \quad (5)$$

According to Rankine's theory, for active case, the angle made by failure plane with the horizontal is given by θ = (45° + ψ/2).

Substitution of Eqs. (3) and (4) into Eq. (5) gives

$$P_d = \frac{0.5\gamma z^2 \cot\left(45°+\frac{\psi}{2}\right)\sqrt{1+k_h^2}\sin\left[45°-\left(\frac{\psi}{2}-\lambda\right)\right]}{\sin\left[45°+\left(\frac{\psi}{2}+\delta\right)\right]} \quad (6)$$

The total seismic active thrust on the wall can be calculated by using Eq. (6).

According to Dubrova's hypothesis, the earth pressure distribution p along the height (z) is obtained by differentiating total earth thrust P_d with respect to z,

$$p = \frac{\partial P_d}{\partial z} = \frac{\partial}{\partial z}\left\{\frac{\gamma z^2\sqrt{1+k_h^2}}{2}\cot\left(45°+\frac{\psi}{2}\right)\frac{\cos\left(\frac{\psi}{2}-\lambda\right)-\sin\left(\frac{\psi}{2}-\lambda\right)}{\cos\left(\frac{\psi}{2}+\delta\right)+\sin\left(\frac{\psi}{2}+\delta\right)}\right\} \quad (7)$$

3.2 Earth Pressure Disrtibution along the Wall for Various Wall Movements

3.2.1 Rotation at Bottom

Equation (7) represents seismic active earth pressure distribution behind the retaining wall. Out of various wall movements, i.e., rotation at the bottom, rotation at the top, and pure translation, initially case of rotation about bottom is considered as shown in Fig. 1(a), where ψ is an orientation angle, given by $\psi = \phi - \phi z/H$. Differentiation gives $\partial\psi/\partial z = -\phi/H$.

Therefore, from Eq. (7), the active earth pressure (p_1) for the case, when wall rotates about its bottom, is given as

$$p_1 = \frac{\partial P_d}{\partial z} = \frac{\gamma\sqrt{1+k_h^2}}{4\sin^2\left(45°+\frac{\psi}{2}\right)\left[\cos\left(\frac{\psi}{2}+\delta\right)+\sin\left(\frac{\psi}{2}+\delta\right)\right]^2} \times\left\{\left(2z\cos\psi+\frac{\phi z^2}{2H}\right)(\cot[\psi-\lambda+\delta]+\sin[\delta+\lambda] + \frac{\phi z^2}{H}\cos\psi\cos[\delta+\lambda]\right\} \quad (8)$$

3.2.2 Rotation at Top

Similarly, when the rotation takes place about the top of the wall as shown in Fig. 1(b), considering ψ as an orientation angle with the normal is given by $\psi = \phi z/H$. Differentiation gives $\partial\psi/\partial z = \phi/H$.

Therefore, from Eq. (7), the active earth pressure (p_2) for the case when the wall rotates about its top is given as

$$p_2 = \frac{\partial P_d}{\partial z} = \frac{\gamma\sqrt{1+k_h^2}}{4\sin^2\left(45°+\frac{\psi}{2}\right)\left[\cos\left(\frac{\psi}{2}+\delta\right)+\sin\left(\frac{\psi}{2}+\delta\right)\right]^2} \times\left\{\left(2z\cos\psi+\frac{\phi z^2}{2H}\right)(\cot[\psi-\lambda+\delta]+\sin[\delta+\lambda] + \frac{\phi z^2}{H}\cos\psi\cos[\delta+\lambda]\right\} \quad (9)$$

3.2.3 Pure Translation

According to Dubrova (1963), pure translation shown in Fig. 1(c) is the combination of both cases, *i.e.,* rotation about bottom and rotation about top. p is the seismic earth pressure distribution in the sliding mode which is the average of two modes, *i.e.,* $p = 0.5\,(p_1 + p_2)$

$$p = \frac{\sqrt{1+k_h^2}\;\gamma\cos\psi z[\cos(\psi-\lambda+\delta)+\sin(\delta+\lambda)]}{2\sin^2\left(45°+\frac{\psi}{2}\right)\left[\cos\left(\frac{\psi}{2}+\delta\right)+\sin\left(\frac{\psi}{2}+\delta\right)\right]^2} \quad (10)$$

Equation (10) gives the value of seismic earth pressure distribution along the height of retaining wall, considering pure translation as wall movement. Equations (8) to (10) are used to determine the seismic active earth pressure distribution behind retaining wall based on modified Dubrova's model.

4. RESULTS AND DISCUSSIONS

Results are presented for normalized seismic active earth pressure ($p_{ae}/\gamma H$) along the normalized depth of the wall (z/H). Variations of parameters considered in the present analysis are as follows: $\phi = 20°$, 25°, 30°, 35° and 40°; $\delta/\phi = 0$, 0.25, 0.5, 0.75 and 1.

4.1 Effect of soil friction angle (ϕ) on static active earth pressure ($k_h = 0$ and $k_v = 0$)

Figure 6 presents normalized static active earth pressure ($p_a / \gamma H$) distribution based on purely translation mode along the normalized depth (z/H) of wall with different values of ϕ, δ, k_h and k_v. It can be interpreted from Figs. 6(a) to 6(e) (with $k_h = 0.0$ and $k_v = 0.0$) that, as soil friction angle (ϕ) increases from 20° to 25°, 25° to 30°, 30° to 35°, and 35° to 40°, there is reduction in static active earth pressure by 17%, 17%, 21%, and 16%, respectively. This is because as the soil friction angle (ϕ) increases, the backfill becomes denser thus reducing the active earth pressure. As ϕ increases from 20° to 40°, the nature of curve changes.

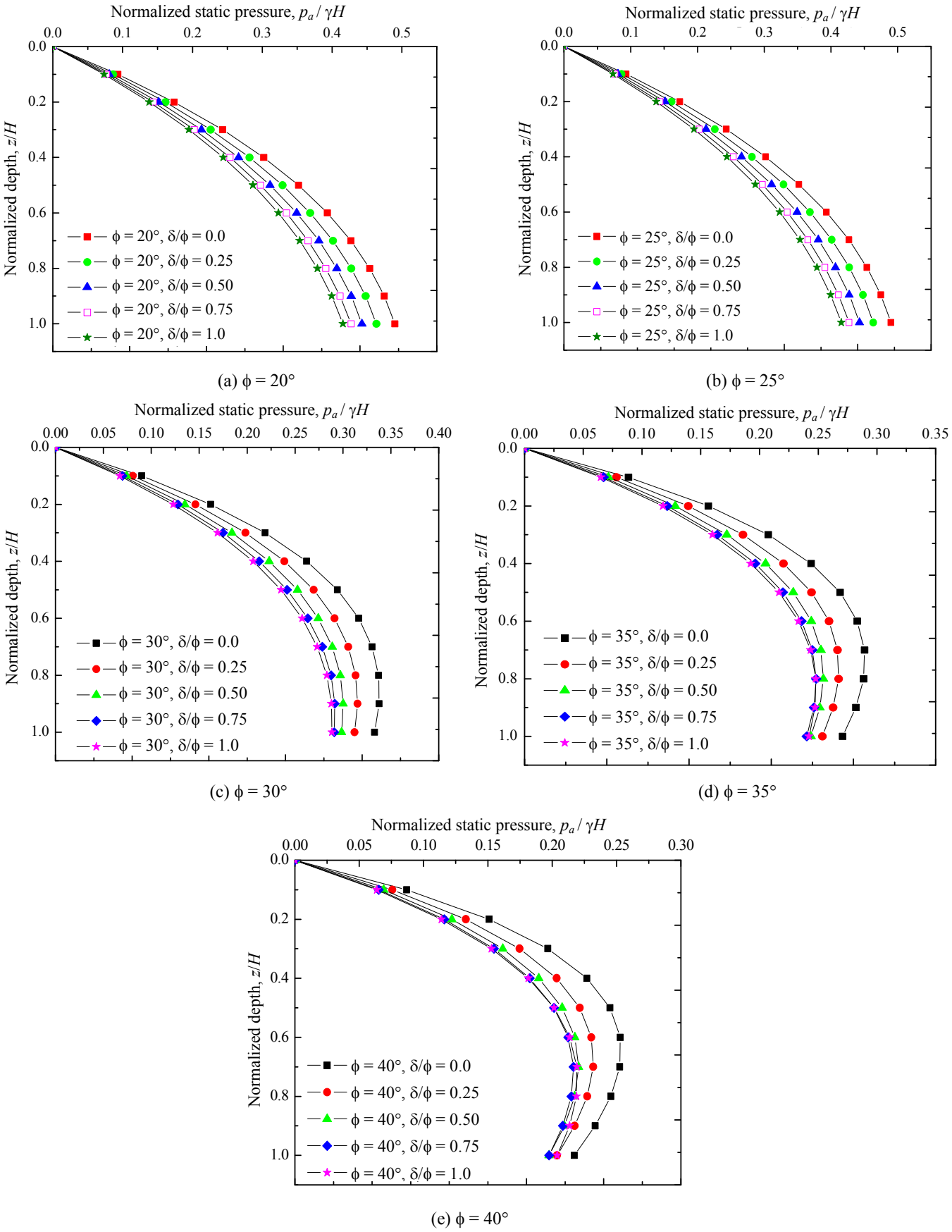

Fig. 6 Variation of normalized static active earth pressure distribution with ($p_a/\gamma H$) normalized depth (z/H) for different values of (ϕ) and (δ) with $k_h = 0$, $k_v = 0$ (translation mode)

4.2 Effect of Seismic Acceleration Coefficients (k_h and k_v) on Seismic Active Earth Pressure

Figure 7 shows typical non-dimensional variation of seismic active earth pressure distribution with depth for different values of seismic acceleration coefficients (k_h and k_v). It is seen from Fig. 7 that with increase in seismic acceleration coefficients, the seismic active earth pressure increases. The seismic values are found to follow a non-linear trend which shows that there is an increase in $p_{ae}/\gamma H$ with increase in the values of z/H. The nonlinearity further increases for higher seismicity. For a given value of seismic vertical acceleration (k_v), when seismic horizontal acceleration (k_h) increases from 0.1 to 0.2, seismic active earth pressure increased by 22%. When k_v increased from 0.25 k_h to 0.5 k_h with k_h = 0.1, there is an increase in seismic active earth pressure by 13%.

This shows that seismic horizontal acceleration has a dominant effect on seismic active earth pressure than that of seismic vertical acceleration. For the constant values of k_h, as k_v increases from 0.25 k_h to 0.75 k_h, the earth pressure curves overlap for both k_h = 0.1 and k_h = 0.2. However, it is necessary to consider the effect of both k_h and k_v in the design of retaining wall.

5. COMPARISON OF RESULTS

The results obtained by the modified Dubrova's model based on redistribution principle (considering seismic effects) are compared with various existing experimental results and analytical methods.

5.1 Comparison of Modified Dubrova's Model with Experimental Results of Tsagareli's method

For checking the validity of the proposed formulation to retaining walls with different heights, predictions from the derived equation are compared with three experimental results. Tsagareli (1965) conducted experiments, in which the distribution of static active earth pressure on translating rigid retaining walls of height 3.0 m was measured. The unit weight of the backfill used in Tsagareli's full-scale tests was 17.65 kN/m^3, backfill soil friction angle (ϕ) = 37°, and wall friction angle (δ) = 28°.

Ying *et al.* (2006) theoretically analyzed the shape of minor principal stress arch considering the effect of soil friction angle on the inclination of the slip plane behind a retaining wall and a partial development of wall friction. Li and Wang (2014) proposed a new method for calculating the active earth pressure acting on a rigid retaining wall that moves horizontally away from soil mass based on the limit-equilibrium concept. Figure 8 shows the comparison of the non-dimensionalized distribution of the active earth pressure evaluated using Eq. (10) with Tsagareli's (1965) wall measurement results. Additionally, Fig. 8 shows the distributions obtained using the analyses of Li and Wang (2014) and Ying *et al.* (2006). It is seen that the results obtained using the proposed formulation are in good agreement with the experimental results.

5.2 Comparison of Modified Dubrova's Model with Experimental Results of Tang's method

Tang (1988) conducted an experiment in which model tests were carried out in a centrifuge. The experimental parameters were as follows: height of the wall (H) = 10 m, unit weight of backfill (γ) = 17.65 kN/m^3, soil friction angle (ϕ) = 30°, and wall friction angle (δ) = 15°. Figure 9 shows the comparison of the non-dimensionalized distributions of the active earth pressure calculated using Eq. (10) with Tang (1988)'s experimental wall measurements. Additionally, Fig. 9 shows the distributions obtained using the analyses of Li and Wang (2014) and Ying *et al.* (2006). Li and Wang (2014) proposed a new method for calculating the active earth pressure acting on a rigid retaining wall that moves horizontally away from soil mass based on the limit-equilibrium concept. Ying *et al.* (2006) theoretically analyzed the shape of minor principal stress arch considering the effect of soil internal friction angle on the inclination of the slip plane. It is observed that the results obtained using the proposed equations are in good agreement with the above mentioned methods.

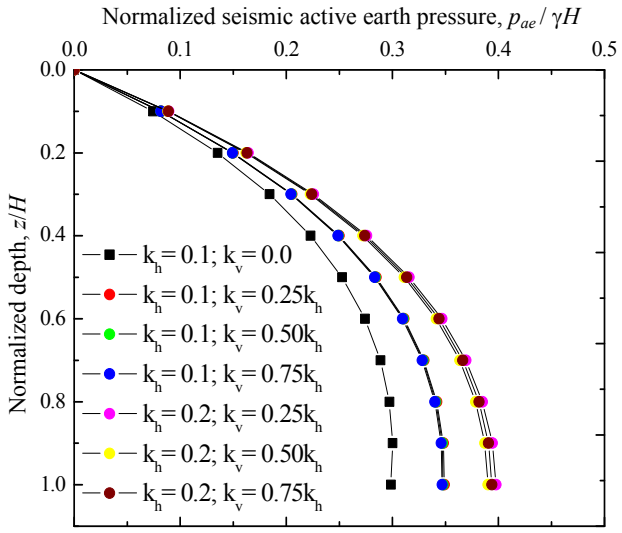

Fig. 7 Typical variation of seismic active earth pressure distribution ($p_{ae}/\gamma H$) for different values of k_h and k_v (with $\delta = \phi/2$ and $\phi = 30°$)

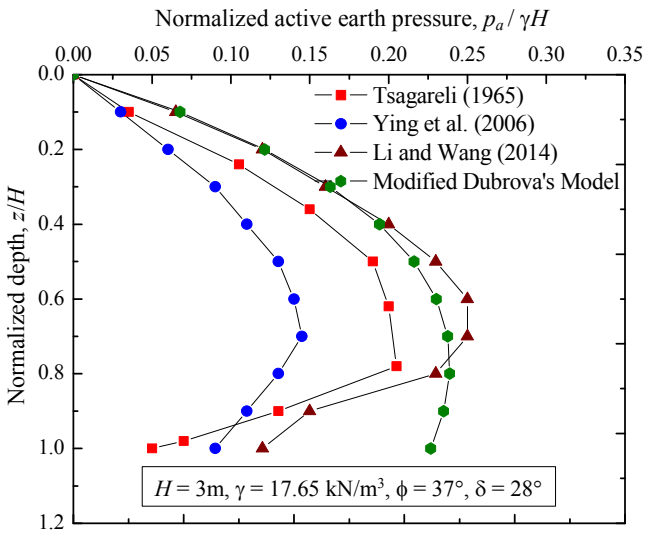

Fig. 8 Validation of Modified Dubrova's model with Tsagareli's method

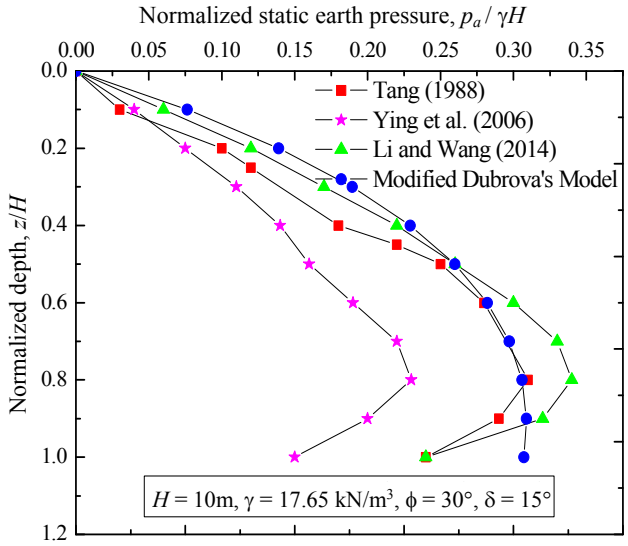

Fig. 9 Validation of modified Dubrova's model with Tang's method

5.3 Comparison of Modified Dubrova's Model with Rao *et al.* (2016)'s Method

To check the applicability of the proposed formulations, the predictions from the derived equation are compared with the experimental results of Tsagareli (1965), in which the distribution of the active earth pressure acting on the 4 m high rigid retaining wall was measured. Tsagareli (1965) states that many works have been devoted to methods of determining earth pressure on a rigid wall with a vertical back face. However, there is no single point of view concerning the stress state of the earth behind the wall, form of the slip surface formed at the moment of limit equilibrium. Rao *et al.* (2016) proposed a new simplified method to compute the active earth pressure acting on the backface of a rigid retaining wall undergoing horizontal translation.

The values of the parameters designed in Tsagareli's full-scale tests are as follows: unit weight of the cohesionless backfill soil (γ) = 18 kN/m³, soil friction angle (ϕ) = 32°, wall friction angle (δ) = 10°, height of the wall (H) = 4 m, and no surcharge load (q = 0) applied on the top of the backfill soil. Figure 10 shows the comparison of the distribution of the active earth pressure calculated using Eq. (10) with the measurements obtained from Tsagareli (1965). The earth pressure obtained using the proposed formulation is 25% higher throughout the height of the wall and is in good agreement with that of Tsagareli theory (1965) and Rao *et al.* (2016)'s method. The above methods capture the salient feature of the nonlinear distribution of active earth pressure, which cannot be predicted by using the existing theories of Coulomb and Rankine.

5.4 Comparison of Modified Dubrova's Model with Ghazavi and Yeganeh (2013)'s Method: Static Case

In order to compare the results obtained from the modified Dubrova's model based on purely translation mode with Ghazavi and Yeganeh (2013)'s method in static case, a rigid retaining wall is considered with a wall height (H) = 3 m, soil friction angle (ϕ) = 30°, wall friction angle (δ) = 0 (smooth wall), and unit weight of backfill material (γ) = 18 kN/m³. The graphical comparison between horizontal earth pressures is made for both methods in the static case as shown in Fig. 11.

As seen in Fig. 11, the distribution of active earth pressure is nonlinear for both methods. For Ghazavi and Yeganeh (2013)'s method, the maximum earth pressure does not occur at the toe of the wall; however, for modified Dubrova's model, the maximum earth pressure occurs at the toe of the wall. The results obtained by the modified Dubrova's method are larger than Ghazavi and Yeganeh (2013)'s results because Ghazavi and Yeganeh (2013) used a plasticity equation to determine the reaction of the stable soil on cohesionless backfill supported by a retaining wall using an empirical equation derived from experiments performed in the field by others.

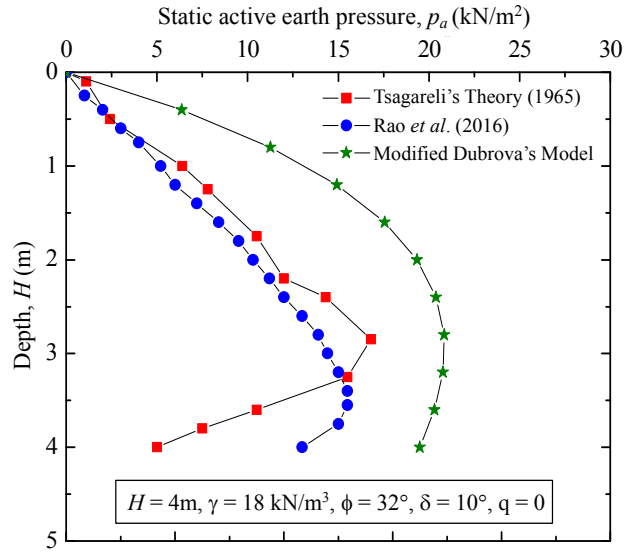

Fig. 10 Comparison between predicted and experimental data

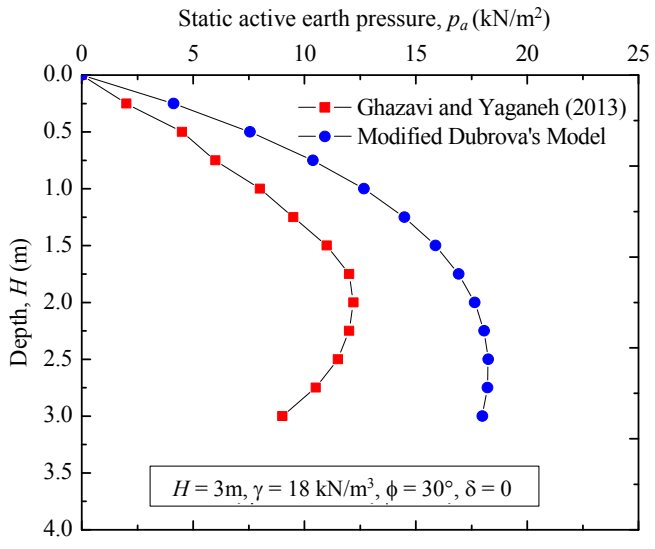

Fig. 11 Distribution of horizontal earth pressure on retaining wall for ϕ = 30°, δ = 0, H = 3 m, and γ = 18 kN/m³

The static earth pressure distribution obtained from the present study is higher by 30% than Ghazavi and Yeganeh (2013)'s method throughout the height of the retaining wall. This is because modified Dubrova's model considers purely the translation mode as a wall movement.

5.5 Comparison of Modified Dubrova's Model with Ghazavi and Yeganeh (2011)'s Method: Seismic Case

In order to compare the results obtained from modified Dubrova's model and Ghazavi and Yeganeh (2011)'s method in seismic case, a rigid retaining wall is considered with wall height (H) = 5 m, soil friction angle (ϕ) = 33°, wall friction angle (δ) = 16°, and unit weight of backfill material (γ) = 18 kN/m^3, with various seismic horizontal acceleration (k_h) = 0.1, 0.2 and 0.3 and seismic vertical acceleration (k_v) = 0. The graphical comparison is made for both methods in seismic case as shown in Fig. 12.

Ghazavi and Yeganeh (2011) presented a solution to compute the seismic earth pressure on the back of a retaining wall on the basis of the limit equilibrium approach and limit state analysis. Ghazavi and Yeganeh (2011) considered equilibrium of forces acting on an element of the failed wedge, and the earth pressure on the wall is obtained using a mathematical procedure. Also, the effect of phase differences in both shear and primary waves travelling through the backfill due to seismic excitation is also considered. As seen in Fig. 12, the earth pressure distribution is nonlinear for both modified Dubrova's approach and Ghazavi and Yeganeh (2011)'s approach.

Its maximum value does not occur at the wall bottom for Ghazavi and Yeganeh (2011)'s approach. Moreover, the earth pressure decreases to zero at the bottom of wall in static nonlinear condition; however, earth pressure is not zero at the bottom of wall in seismic condition with various k_h for both Ghazavi and Yeganeh (2011)'s and modified Dubrova's models. This indicates that seismic active earth pressure obtained from modified Dubrova's model must be considered in the design at the bottom of the wall.

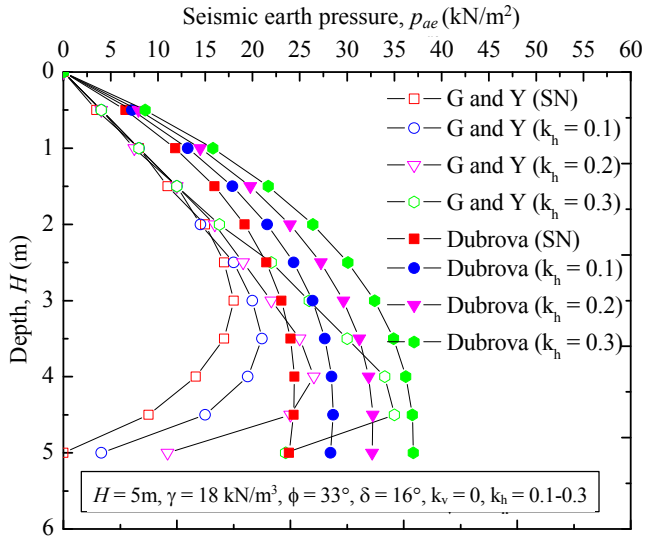

Fig. 12 Distribution of horizontal earth pressure on retaining wall for ϕ = 33°, δ = 16°, k_h = 0.1 to 0.3, k_v = 0, H = 5 m, and γ = 18 kN/m^3 (G and Y = Ghazavi and Yeganeh, SN = static nonlinear)

5.6 Comparison of Modified Dubrova's Model with Goel and Patra (2008)'s Method for different δ/ϕ

Figure 13 presents the variation of lateral earth pressure along the depth of the retaining wall for two ratios (δ/ϕ = 0.75 and 1.0). The lateral active earth pressure has been non-dimensionalized with respect to wall height (H) and the unit weight of backfill soil (γ). The depth coordinate along the wall height (z) has been non dimensionalized with respect to the wall height (H).

The present study is compared with Goel and Patra (2008) for δ/ϕ = 0.75 and 1. Goel and Patra (2008) presented various combinations of shapes of critical failure surface, and arch shapes were studied to estimate the coefficient of active earth pressure on the rigid retaining wall in cohesionless soil. It is found that both studies give the nonlinear distribution of the static earth pressure. For Goel and Patra (2008), earth pressure is not maximum at the toe, whereas the present study shows earth pressure is maximum at the toe. This is because the present model is developed based on pure translation mode.

Figure 13 clearly brings out the nonlinear nature of variation of static active earth pressure for varying δ/ϕ ratios. This is consistent with Terzaghi (1943)'s prediction of nonlinear variation of earth pressure along the wall height.

5.7 Comparison of Modified Dubrova's Model with Wang *et al.* (2004)'s Method

Figure 14 shows the distribution of the lateral earth pressure on a retaining wall considering wall movement in terms of translation and rotation about top for the soil friction angle ϕ = 36° and wall friction angle $\delta = \phi/2$ (Wang *et al.* 2004). It is seen from Fig. 14 that there is a significant difference in the distributions of the lateral earth pressure for the wall movement mode of translation (T), rotation about the top (RT), and the linear distribution. Wang *et al.* (2004) is based on the Coulomb's theory that the earth pressure against the back of a retaining wall is due to

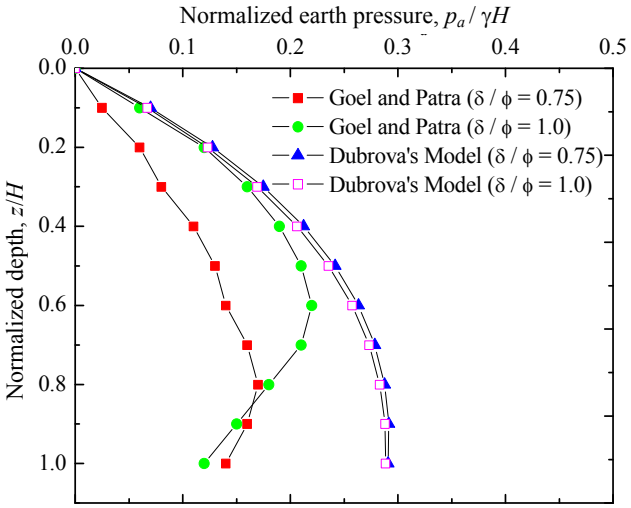

Fig. 13 Variation of active lateral earth pressure force with wall height for different δ/ϕ

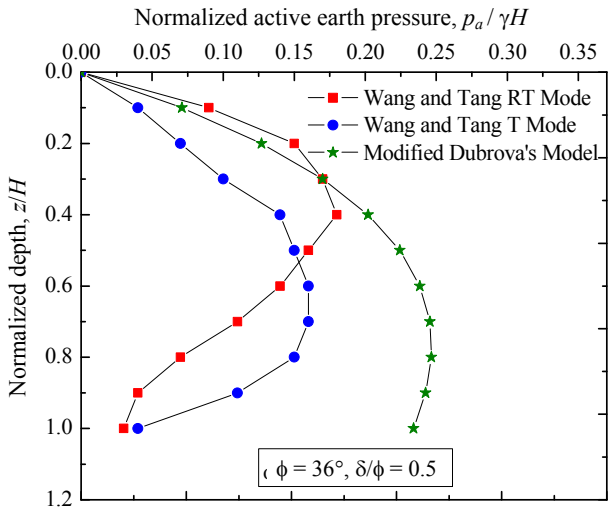

Fig. 14 Distribution of earth pressure for various wall movements (RT: Rotation at the top mode and T: Purely translation mode)

the thrust exerted by the sliding wedge of soil from the back of the wall. For Wang *et al.* (2004)'s approach, the position of maximum earth pressure for the wall movement mode of translation is approximately at $0.35H \sim 0.40H$ above the wall base, and the position of maximum earth pressure for the wall movement mode of rotation about top is approximately at $0.60H \sim 0.70H$ above the wall base, which is higher than that for the wall movement mode of translation.

6. SUMMARY AND CONCLUSIONS

The study presents the distribution of lateral earth pressures due to static and seismic loading behind rigid retaining walls using a closed form solution. The present study considers both static and seismic earth pressure distributions in a nonlinear manner. In this study, the mathematical model is proposed to determine the nonlinear distribution of the active earth pressure acting on translating retaining wall by considering various modes of the wall movement. Comparisons between different analytical and experimental results show that the modified Dubrova's model yields satisfactory results. There are significant differences in the points of application of the resultant earth pressure for various modes of wall movement. The important conclusions drawn from the study are presented below.

When rotation at bottom takes place, seismic earth pressure by modified Dubrova's model is highest, and also distribution is nonlinear. When rotation at top takes place, the seismic earth pressure by modified Dubrova's model is higher than existing methods, and also distribution is parabolic. On the other hand, if there is a purely translation mode, seismic earth pressure by modified Dubrova's model is approximately the same as that of existing methods, and also distribution is parabolic.

Thus, the distributions of active earth pressures on a rigid retaining wall are nonlinear and are different for different modes of wall movement. In the present analysis, the point of application of the resultant earth pressure is approximately at $0.35H \sim 0.40H$ above the wall base as the wall movement mode is purely translation. Results obtained using modified Dubrova's model is in good agreement with the experimental results of Tsagareli, Tang, Li and Wang, and Ying *et al.* Without surcharge loading, earth pressure obtained by modified Dubrova's model is 25% higher than that of Rao and Chen's study. Though seismic earth pressure obtained by all approaches studied and the seismic earth pressures obtained by modified Dubrova's model have different assumptions, the final nonlinear earth pressure distribution is approximately same.

NOTATIONS

p_a	Static active earth pressure (kN/m^2)
p_{ae}	Seismic active earth pressure (kN/m^2)
P_d	Active earth pressure thrust (kN/m)
p_1	Seismic earth pressure distribution when the retaining wall rotates about bottom (kN/m^2)
p_2	Seismic earth pressure distribution when the retaining wall rotates about top (kN/m^2)
P	Seismic earth pressure distribution when the retaining wall is in purely sliding mode (kN/m^2)
$p_a/\gamma H$	Normalized static active earth pressure
$p_{ae}/\gamma H$	Normalized seismic active earth pressure
k_h	Horizontal acceleration coefficient
k_v	Vertical acceleration coefficient
Δ	Wall friction angle (°)
ϕ	Soil friction angle (°)
ψ	Orientation angle (°)
z/H	Normalized depth

REFERENCES

Bang, S. (1985). "Active earth pressure behind retaining walls." *Journal of Geotechnical Engineering*, ASCE, **111**(3), 407-412. https://doi.org/10.1061/(ASCE)0733-9410(1985)111:3(407)

Choudhury, D., Katdare, A.D., and Pain, A. (2014). "New method to compute seismic active earth pressure on retaining wall considering seismic waves." *Journal of Geotechnical and Geological Engineering*, **32**(2), 391-402. https://doi.org/10.1007/s10706-013-9721-8

Choudhury, D. and Nimbalkar, S. (2006). "Pseudo-dynamic approach of seismic active earth pressure behind retaining wall." *Journal of Geotechnical and Geological Engineering*, **24**(5), 1103-1113. https://doi.org/10.1007/s10706-005-1134-x

Choudhury, D. and Singh, S. (2006). "New approach for estimation of static and seismic active earth pressure." *Journal of Geotechnical and Geological Engineering*, **24**(1), 117-127. https://doi.org/10.1007/s10706-004-2366-x

Coulomb, C.A. (1776). "Essai sur une application des regles de maximis et minimize a quelqes problemes de stratique relatifs a l' architecture." *Memoires de mathematique et de physique, Presentes a l' academie royale des science* (Mem. Acad. Roy. Div. Sav.), **7**, 343-387.

Das, B.M. (2007). *Principles of Foundation Engineering*, 6th Ed., Thomson.

Dubrova, G.A. (1963). *Interaction between Soils and Structures*. Rechnoi Transport (in Russian).

Fang, Y. and Ishibashi, I. (1986). "Static earth pressures with various wall movements." *Journal of Geotechnical Engineering*, ASCE, **112**(3), 317-333. https://doi.org/10.1061/(ASCE)0733-9410(1986)112:3(317)

Ghazavi, M. and Yeganeh, M. (2013). "Mathematical analysis of lateral earth pressure distribution on rigid retaining walls."

Journal of Engineering Geology, **6**(2), 1459-1474.
Goel, S. and Patra, N.R. (2008). "Effect of arching on active earth pressure for rigid retaining walls considering translation mode." *International Journal of Geomechanics*, ASCE, **8**(2), 123-133. https://doi.org/10.1061/(ASCE)1532-3641(2008)8:2(123)
Harr, M. E. (1966). *Foundations of Theoretical Soil Mechanics*, McGraw Hill Book Company.
Kramer, S. L. (1996). *Geotechnical Earthquake Engineering*, Prentice Hall, Upper Saddle River, N.J. https://doi.org/10.1007/s10518-013-9484-x
Li, J. P. and Wang, M. (2014). "Simplified method for calculating active earth pressure on rigid retaining walls considering the arching effect under translational mode." *International Journal of Geomechanics*, ASCE, **14**(2), 282-290. https://doi.org/10.1061/(ASCE)GM.1943-5622.0000313
Mononobe, N. and Matsuo, H. (1929). "On the determination of earth pressures during earthquakes." *Proceeding of World Engineering Congress,* **9**, 177-185.
Okabe, S. (1924). "General theory on earth pressure and seismic stability of retaining wall and dam." *Journal of the Japanese Society of Civil Engineering*, **10**(6), 1277-1323.
Rao, P., Chen, Q., Zhou, Y., and Nimbalkar, S. (2016). "Determination of active earth pressure on rigid retaining wall considering arching effect in cohesive backfill soil." *International Journal of Geomechanics*, ASCE, **16**(3), 821-829. https://doi.org/10.1061/(ASCE)GM.1943-5622.0000589
Richards, R. and Shi, X. (1994). "Seismic lateral pressures in soils with cohesion." *Journal of Geotechnical Engineering*, ASCE, **120**(7), 1230-1251. https://doi.org/10.1061/(ASCE)0733-9410(1994)120:7(1230)
Subba Rao, K. S. and Choudhury, D. (2005). "Seismic passive earth pressures in soils." *Journal of Geotechnical and Geoenvironmental Engineering*, ASCE, **131**(1), 131-135. https://doi.org/10.1061/(ASCE)1090-0241(2005)131:1(131)
Tang, Z.C. (1988). "A rigid retaining wall centrifuge model test of cohesive soil." *Journal of Chongqing Jiaotong University,* **25**(2), 48-56.
Terzaghi, K. (1943). *Theoretical Soil Mechanics.* John Wiley and Sons, New York, NY, USA. https://doi.org/10.1002/9780470172766
Tsagareli, Z.V. (1965). "Experimental investigation of the pressure of a loose medium on retaining walls with a vertical back face and horizontal backfill surface." *Journal of Soil Mechanics and Foundation Engineering*, **91**(4), 197-200. https://doi.org/10.1007/BF01706095
Wang, Y.Z., Tang, Z.P., and Zheng, B. (2004). "Distribution of active earth pressure of retaining wall with wall movement of rotation about top." *Applied Mathematics and Mechanics*, **25**(7) 761-767. https://doi.org/10.1007/BF02437567
Ying, H.W., Jiang, B., and Xie, K.H. (2006). "Parallel to the vertical wall of soil arching effect of lateral soil pressure." *Journal of Hydraulic Engineering*, **37**(11), 1303-1308 (in Chinese).

APPENDIX

A detailed formulation, explaining how to combine two modes of wall movements into the transitional movement, is presented. The total seismic active earth thrust (P_d) is given by Eq. (6). Differentiating above Eq. (6) gives seismic active earth pressure distribution p:

$$p=\frac{\partial P_d}{\partial z}=\frac{\partial}{\partial z}\left\{\frac{\gamma z^2\sqrt{1+k_h^2}}{2}\cot\left(45°+\frac{\psi}{2}\right)\frac{\cos\left(\frac{\psi}{2}-\lambda\right)-\sin\left(\frac{\psi}{2}-\lambda\right)}{\cos\left(\frac{\psi}{2}+\delta\right)+\sin\left(\frac{\psi}{2}+\delta\right)}\right\} \tag{A1}$$

Putting, $\psi=\phi-\frac{\phi z}{H}$. Differentiating, $\frac{\partial\psi}{\partial z}=-\frac{\phi}{H}$

$$p=\left\{\frac{2\gamma z\sqrt{1+k_h^2}}{2}\cot\left(45°+\frac{\psi}{2}\right)\frac{\cos\left(\frac{\psi}{2}-\lambda\right)-\sin\left(\frac{\psi}{2}-\lambda\right)}{\cos\left(\frac{\psi}{2}+\delta\right)+\sin\left(\frac{\psi}{2}+\delta\right)}\right\}$$

$$+\left\{-\csc^2\left(45°+\frac{\psi}{2}\right)\cdot\left(\frac{-\phi}{2H}\right)\frac{\gamma z^2\sqrt{1+k_h^2}}{2}\cdot\frac{\cos\left(\frac{\psi}{2}-\lambda\right)-\sin\left(\frac{\psi}{2}-\lambda\right)}{\cos\left(\frac{\psi}{2}+\delta\right)+\sin\left(\frac{\psi}{2}+\delta\right)}\right\}$$

$$+\left\{\frac{\gamma z^2\sqrt{1+k_h^2}}{2}\cot\left(45°+\frac{\psi}{2}\right)\left[\frac{\left\{\cos\left(\frac{\psi}{2}+\delta\right)+\sin\left(\frac{\psi}{2}+\delta\right)\right\}\cdot\left\{-\sin\left(\frac{\psi}{2}-\lambda\right)\left(\frac{-\phi}{2H}\right)-\cos\left(\frac{\psi}{2}-\lambda\right)\left(\frac{-\phi}{2H}\right)\right\}}{\left\{-\cos\left(\frac{\psi}{2}-\lambda\right)-\sin\left(\frac{\psi}{2}-\lambda\right)\right\}\cdot\left\{-\sin\left(\frac{\psi}{2}+\delta\right)\left(\frac{-\phi}{2H}\right)+\cos\left(\frac{\psi}{2}+\delta\right)\left(\frac{-\phi}{2H}\right)\right\}}{\cos\left(\frac{\psi}{2}+\delta\right)+\sin\left(\frac{\psi}{2}+\delta\right)}\right]\right\} \quad \text{(A2)}$$

$$A=\gamma z\sqrt{1+k_h^2}\cdot\frac{\cos\left(45°+\frac{\psi}{2}\right)\cdot\sin\left(45°+\frac{\psi}{2}\right)}{\sin^2\left(45°+\frac{\psi}{2}\right)}\frac{\left[\cos\left(\frac{\psi}{2}-\lambda\right)-\sin\left(\frac{\psi}{2}-\lambda\right)\right]\left[\cos\left(\frac{\psi}{2}+\delta\right)-\sin\left(\frac{\psi}{2}+\delta\right)\right]}{\left\{\cos\left(\frac{\psi}{2}+\delta\right)+\sin\left(\frac{\psi}{2}+\delta\right)\right\}^2}\cdot\frac{4}{4}$$

$$A=\frac{\gamma\sqrt{1+k_h^2}}{4\sin^2\left(45°+\frac{\psi}{2}\right)}\cdot\frac{2z\sin(90°+\psi)}{\left\{\cos\left(\frac{\psi}{2}+\delta\right)+\sin\left(\frac{\psi}{2}+\delta\right)\right\}^2}\left[\begin{array}{l}\cos\left(\frac{\psi}{2}-\lambda\right)\cdot\cos\left(\frac{\psi}{2}+\delta\right)-\sin\left(\frac{\psi}{2}-\lambda\right)\cdot\sin\left(\frac{\psi}{2}+\delta\right)+\\ \cos\left(\frac{\psi}{2}-\lambda\right)\cdot\sin\left(\frac{\psi}{2}+\delta\right)-\sin\left(\frac{\psi}{2}-\lambda\right)\cdot\cos\left(\frac{\psi}{2}+\delta\right)\end{array}\right]$$

$$A=\frac{\gamma\sqrt{1+k_h^2}}{4\sin^2\left(45°+\frac{\psi}{2}\right)}\cdot\frac{2z\sin(90°+\psi)}{\left\{\cos\left(\frac{\psi}{2}+\delta\right)+\sin\left(\frac{\psi}{2}+\delta\right)\right\}^2}\cdot\left[\cos(\psi+\delta-\lambda)+\sin(\lambda+\delta)\right] \quad \text{(A3)}$$

$$B=\frac{\phi}{4H}\cdot\frac{1}{\sin^2\left(45°+\frac{\psi}{2}\right)}\cdot\gamma z^2\sqrt{1+k_h^2}\cdot\frac{\left[\cos\left(\frac{\psi}{2}-\lambda\right)-\sin\left(\frac{\psi}{2}-\lambda\right)\right]\left[\cos\left(\frac{\psi}{2}+\delta\right)-\sin\left(\frac{\psi}{2}+\delta\right)\right]}{\left\{\cos\left(\frac{\psi}{2}+\delta\right)+\sin\left(\frac{\psi}{2}+\delta\right)\right\}^2}$$

$$B=\frac{\gamma\sqrt{1+k_h^2}}{4\sin^2\left(45°+\frac{\psi}{2}\right)}\cdot\frac{\frac{\phi z^2}{H}}{\left\{\cos\left(\frac{\psi}{2}+\delta\right)+\sin\left(\frac{\psi}{2}+\delta\right)\right\}^2}\cdot\left[\begin{array}{l}\cos\left(\frac{\psi}{2}-\lambda\right)\cdot\cos\left(\frac{\psi}{2}+\delta\right)-\sin\left(\frac{\psi}{2}-\lambda\right)\cdot\sin\left(\frac{\psi}{2}+\delta\right)+\\ \cos\left(\frac{\psi}{2}-\lambda\right)\cdot\sin\left(\frac{\psi}{2}+\delta\right)-\sin\left(\frac{\psi}{2}-\lambda\right)\cdot\cos\left(\frac{\psi}{2}+\delta\right)\end{array}\right]$$

$$B=\frac{\gamma\sqrt{1+k_h^2}}{4\sin^2\left(45°+\frac{\psi}{2}\right)}\cdot\frac{\frac{\phi z^2}{H}}{\left\{\cos\left(\frac{\psi}{2}+\delta\right)+\sin\left(\frac{\psi}{2}+\delta\right)\right\}^2}\cdot\left[\cos(\psi+\delta-\lambda)+\sin(\lambda+\delta)\right] \quad \text{(A4)}$$

$$C=\frac{\gamma z^2\sqrt{1+k_h^2}}{2}\cdot\frac{\cos\left(45°+\frac{\psi}{2}\right)\cdot\sin\left(45°+\frac{\psi}{2}\right)}{\sin^2\left(45°+\frac{\psi}{2}\right)}\cdot\frac{\left\{\begin{bmatrix}\frac{\phi}{2H}\cdot\cos\left(\frac{\psi}{2}+\delta\right)\cdot\sin\left(\frac{\psi}{2}-\lambda\right)+\frac{\phi}{2H}\cdot\cos\left(\frac{\psi}{2}+\delta\right)\cdot\cos\left(\frac{\psi}{2}-\lambda\right)\\+\frac{\phi}{2H}\cdot\sin\left(\frac{\psi}{2}+\delta\right)\cdot\sin\left(\frac{\psi}{2}-\lambda\right)+\frac{\phi}{2H}\cdot\sin\left(\frac{\psi}{2}+\delta\right)\cdot\cos\left(\frac{\psi}{2}-\lambda\right)\end{bmatrix}-\right.}{\left\{\cos\left(\frac{\psi}{2}+\delta\right)+\sin\left(\frac{\psi}{2}+\delta\right)\right\}^2}$$

$$\left.\begin{bmatrix}\frac{\phi}{2H}\cdot\cos\left(\frac{\psi}{2}-\lambda\right)\cdot\sin\left(\frac{\psi}{2}+\delta\right)-\frac{\phi}{2H}\cdot\cos\left(\frac{\psi}{2}-\lambda\right)\cdot\cos\left(\frac{\psi}{2}+\delta\right)\\-\frac{\phi}{2H}\cdot\sin\left(\frac{\psi}{2}-\lambda\right)\cdot\sin\left(\frac{\psi}{2}+\delta\right)+\frac{\phi}{2H}\cdot\sin\left(\frac{\psi}{2}-\lambda\right)\cdot\cos\left(\frac{\psi}{2}+\delta\right)\end{bmatrix}\right\}$$

$$C=\frac{\gamma\sqrt{1+k_h^2}}{4\sin^2\left(45°+\frac{\psi}{2}\right)}\cdot\frac{\frac{\phi z^2}{H}\cdot\sin(90°+\psi)}{\left\{\cos\left(\frac{\psi}{2}+\delta\right)+\sin\left(\frac{\psi}{2}+\delta\right)\right\}^2}\cdot\left[\cos\left(\frac{\psi}{2}+\delta-\frac{\psi}{2}+\lambda\right)+\cos\left(\frac{\psi}{2}+\delta-\frac{\psi}{2}+\lambda\right)\right]$$

$$C=\frac{\gamma\sqrt{1+k_h^2}}{4\sin^2\left(45°+\frac{\psi}{2}\right)}\cdot\frac{\frac{\phi z^2}{H}\cdot\sin(90°+\psi)}{\left\{\cos\left(\frac{\psi}{2}+\delta\right)+\sin\left(\frac{\psi}{2}+\delta\right)\right\}^2}\cdot\left[2\cos(\delta+\lambda)\right] \tag{A5}$$

$$p=\frac{\partial P_d}{\partial z}=A+B+C \tag{A6}$$

In the Dubrova (1963), seismic earth pressure distribution depends on the various modes of wall movements, *i.e.,* rotation at the bottom, rotation at the top, and pure translation mode. As retaining wall rotates at the bottom ($\psi=\phi-\phi z/H$), the seismic earth pressure distribution is given by

$$p=\frac{\partial P_d}{\partial z}=\frac{\gamma\sqrt{1+k_h^2}}{4\sin^2\left(45°+\frac{\psi}{2}\right)\left[\cos\left(\frac{\psi}{2}+\delta\right)+\sin\left(\frac{\psi}{2}+\delta\right)\right]^2}\cdot\left\{\left(2z\cos\psi+\frac{\phi z^2}{H}\right)\left(\cos[\psi-\lambda+\delta]+\sin[\delta+\lambda]\right)+\frac{2\phi z^2}{H}\cos\psi\cos[\delta+\lambda]\right\} \tag{A7}$$

As retaining wall rotates at the top ($\psi=\phi z/H$), the seismic earth pressure distribution is given by

$$p_2=\frac{\partial P_d}{\partial z}=\frac{\gamma\sqrt{1+k_h^2}}{4\sin^2\left(45°+\frac{\psi}{2}\right)\left[\cos\left(\frac{\psi}{2}+\delta\right)+\sin\left(\frac{\psi}{2}+\delta\right)\right]^2}\cdot\left\{\left(2z\cos\psi+\frac{\phi z^2}{H}\right)\left(\cos[\psi-\lambda+\delta]+\sin[\delta+\lambda]\right)+\frac{2\phi z^2}{H}\cos\psi\cos[\delta+\lambda]\right\} \tag{A8}$$

Dubrova (1963) assumed seismic earth pressure distribution in the sliding mode (p) is the average of above two modes, *i.e.,* $p=\frac{1}{2}(p_1+p_2)$, and is given by

$$p=\frac{\sqrt{1+k_h^2}\,\gamma\cos\psi z\left[\cos(\psi-\lambda+\delta)+\sin(\delta+\lambda)\right]}{2\sin^2\left(45°+\frac{\psi}{2}\right)\left[\cos\left(\frac{\psi}{2}+\delta\right)+\sin\left(\frac{\psi}{2}+\delta\right)\right]^2} \tag{A9}$$